NASA TM X-331

TECHNICAL MEMORANDUM

X-331

LOW-SPEED FLIGHT CHARACTERISTICS OF REENTRY VEHICLES OF THE GLIDE-LANDING TYPE

By John W. Paulson, Robert E. Shanks,
and Joseph L. Johnson

Langley Research Center
Langley Field, Va.

NATIONAL AERONAUTICS AND SPACE ADMINISTRATION

WASHINGTON

NATIONAL AERONAUTICS AND SPACE ADMINISTRATION

TECHNICAL MEMORANDUM X-331

LOW-SPEED FLIGHT CHARACTERISTICS OF REENTRY VEHICLES OF THE GLIDE-LANDING TYPE*

By John W. Paulson, Robert E. Shanks,
and Joseph L. Johnson

SUMMARY

A low-speed investigation has been made to determine the flight characteristics of a number of reentry vehicles of the glide-landing type. The investigation consisted of model flight tests, static and dynamic force tests, and analytical studies of the dynamic lateral behavior over an angle-of-attack range from 0° to 40°.

The longitudinal characteristics for glide landings should be satisfactory with the lift-drag ratios and wing loadings now being considered for reentry configurations. The lateral stability characteristics should also be satisfactory except that many of the reentry vehicles are likely to require a roll damper for satisfactory Dutch-roll damping at moderate and high angles of attack. Some configurations with wing-tip vertical tails may have control problems in the form of large adverse aileron yawing moments and low rudder effectiveness.

INTRODUCTION

Reference 1 covers some of the factors involved in the final approach and landing of reentry vehicles. The present paper gives additional information on this subject which includes data obtained from force tests and flight tests of models of a number of specific reentry configurations. The first part of the paper covers longitudinal characteristics, including lift-drag ratio, aerodynamic-center location, and the effect of center-of-gravity location on longitudinal behavior. The second part consists of a discussion of lateral stability and control. Although it is anticipated that the reentry vehicles considered in this paper would not normally be operated at angles of attack greater than about 15° or 20° in the glide approach and landing, the characteristics over a much larger angle-of-attack range are covered to provide information that would be of interest in cases where higher angles of attack are reached inadvertently.

[redacted]

SYMBOLS

b	wing span, ft
$\bar{c}$	mean aerodynamic chord, ft
C_L	lift coefficient, $\frac{\text{Lift}}{qS}$
C_l	rolling-moment coefficient, $\frac{\text{Rolling moment}}{qSb}$
C_m	pitching-moment coefficient, $\frac{\text{Pitching moment}}{qS\bar{c}}$
C_n	yawing-moment coefficient, $\frac{\text{Yawing moment}}{qSb}$
D	drag, lb
g	acceleration due to gravity, ft/sec^2
I_X	moment of inertia about X-axis, slug-ft^2
I_Z	moment of inertia about Z-axis, slug-ft^2
L	lift, lb
p	rolling velocity, radians/sec
q	dynamic pressure, lb/sq ft; pitching velocity, radians/sec
r	yawing velocity, radians/sec
S	wing area, sq ft
$T_{1/2}$	time to damp to one-half amplitude, sec
V	free-stream velocity, ft/sec
W	weight, lb
α	angle of attack, deg

[redacted]

β angle of sideslip, deg

$\dot{\beta} = \frac{\partial \beta}{\partial t}$

δ_a aileron deflection, deg

δ_r rudder deflection, deg

ω angular velocity, radians/sec

$C_{n_\beta} = \frac{\partial C_n}{\partial \beta}$ $\quad C_{l_\beta} = \frac{\partial C_l}{\partial \beta}$

$C_{n_{\delta_a}} = \frac{\partial C_n}{\partial \delta_a}$ $\quad C_{l_{\delta_a}} = \frac{\partial C_l}{\partial \delta_a}$

$C_{n_{\delta_r}} = \frac{\partial C_n}{\partial \delta_r}$ $\quad C_{n_r} = \frac{\partial C_n}{\partial \frac{rb}{2V}}$

$C_{l_{\dot{\beta}}} = \frac{\partial C_l}{\partial \frac{\dot{\beta} b}{2V}}$ $\quad C_{l_p} = \frac{\partial C_l}{\partial \frac{pb}{2V}}$

$C_{n_p} = \frac{\partial C_n}{\partial \frac{pb}{2V}}$ $\quad C_{m_q} = \frac{\partial C_m}{\partial \frac{q\bar{c}}{2V}}$

Subscripts:

MAX maximum

DYN dynamic

RESULTS AND DISCUSSION

Longitudinal Characteristics

Presented in figure 1 is the approximate range of the low-speed maximum trimmed lift-drag ratio as a function of lift coefficient for various reentry vehicles of the glide-landing type currently under

consideration. The figure shows that some reentry vehicles can have fairly high values of L/D, and the maximum L/D values occur at relatively low lift coefficients of 0.2 to 0.3.

One of the reasons for the large spread in L/D values is shown in figure 2 where maximum L/D is plotted as a function of a nondimensional volume parameter (volume to the two-thirds power divided by wing area). In this figure the nose of each model corresponds to its test point. The results shown are for trimmed conditions and a small amount of longitudinal stability. This figure shows that the higher values of L/D are associated with the winged glide-landing configurations and the lower values of L/D are associated with the lifting-body configurations which would have to be landed with a parachute. The data of figure 2 were obtained at low Reynolds numbers; a few tests at higher Reynolds numbers have indicated that L/D values for the corresponding full-scale reentry vehicle may be as much as 0.5 to 1.0 greater than these values. The configurations illustrated in figure 2 were all designed for the hypersonic condition and for the most part have rather low L/D values at subsonic speeds.

Figure 3 shows that substantial increases in subsonic L/D values can be attained when some effort is also made to design the vehicle for the low-speed case. The shaded area represents the region in which the maximum L/D values for the configurations of figure 2 were located. Boattailing the base of the half-cone and pyramid-shaped vehicles increased the L/D values from about 1.5 to 3.8 and from about 3 to 5, respectively. Adding control surfaces to the half-cone vehicle resulted in a further increase to about 4.5. In the case of the winged reentry configuration with the volume ratio of 0.25, an L/D of about 6 was obtained when the model was modified to achieve high L/D at low speeds. With these modifications, the model had a thick, highly cambered wing and teardrop fuselage with a low base area. The hypersonic L/D of this model was reduced by these changes, but the hypersonic L/D values for the half-cone and pyramid-shaped vehicles were relatively unaffected by boattailing. Another method for obtaining good L/D for landing is the use of a variable-geometry vehicle such as the one at the top of figure 3. This configuration has wing tips that are folded up to protect them from high heating rates during reentry at high angles of attack. For landing, the surfaces are folded down and L/D values of about 7 are obtained.

In order to compare the L/D of some of these configurations with those of the research airplanes discussed in reference 1, figure 4 is presented. In this figure the values of L/D for the variable-geometry configuration, the modified half-cone vehicle, and a winged reentry vehicle are given along with values of L/D for the X-15 airplane and for the modified F-102A airplane with landing gear and speed brakes

extended. Data are shown for the low-wing-loading and high-wing-loading cases. The modified F-102A airplane with a maximum L/D of about 3.7 and a wing loading of 35 was satisfactory in the landing approach (ref. 1). It would appear then that the two low-wing-loading reentry configurations would be satisfactory since they have higher values of L/D, particularly at the lower lift coefficients, and also somewhat lower wing loadings than the modified F-102A airplane. These low wing loadings (in the range of 20 to 30) are typical for winged reentry vehicles. A reentry vehicle that is essentially a lifting body, such as the half-cone configuration, will have a much higher wing loading than a winged vehicle having the same volume. For the higher wing-loading case, a comparison is made with the X-15 airplane which was found to have acceptable landing characteristics. The X-15 airplane performs the approach and landing in the low-lift-coefficient range (about 0.2 to 0.4). It would appear that the half-cone configuration, which has a higher L/D in the 0.2 to 0.4 lift-coefficient range and a slightly lower wing loading than the X-15 airplane, would also have satisfactory landing characteristics.

Another low-speed characteristic of interest to the designer of a hypersonic vehicle is the aerodynamic-center location which must, of course, be aft of the center of gravity for longitudinal stability. Shown in figure 5 is the variation of the aerodynamic-center location with leading-edge sweep for thin-flat-plate delta wings. It is seen that there is a systematic variation in aerodynamic-center position with sweep approaching the theoretical value of 50 percent at 90° sweep. Also shown are the aerodynamic-center locations for several reentry vehicles as given by symbols showing their cross-sectional views. These data indicate that a rearward (or stabilizing) shift in aerodynamic center generally results when the wing is very thick, when a large fuselage is added, or when wing-tip vertical tails are used.

Longitudinal flight characteristics obtained with a highly swept delta-wing flying model, which is considered to be generally representative of highly swept reentry vehicles, is presented in figure 6. Plotted in this figure are flight ratings, as shown by the shaded areas, for various combinations of damping in pitch C_{m_q} and static longitudinal stability. The vertical line is the boundary between the statically stable condition and the unstable condition, and the diagonal line represents the calculated stick-fixed maneuver point. The maneuver point is that center-of-gravity position where the elevator deflection per g is zero. The maneuver-point line has a slope because the maneuver point is a function of damping in pitch and moves rearward as pitch damping is increased. The lower curve represents the model without pitch damper. These studies showed that for all statically stable conditions the model was easy to fly. As pitch damping was added, good flight behavior could also be obtained with statically unstable conditions. As the maneuver point was approached for any condition of pitch

damping, the model became more difficult to fly and finally became unflyable. The flight tests also showed that when reduced elevator deflection was used, the model could not be flown with as much instability as shown in figure 6; this effect indicated that, to some extent at least, the amount of instability which could be tolerated was a function of the total pitching moment used for control.

These model flight results are in general agreement with analog studies (ref. 2) and with flight studies made with conventional airplanes (ref. 3).

Lateral Characteristics

Presented in figure 7 is the variation with sweep angle of the effective-dihedral parameter C_{l_β}, the steady-state damping-in-roll parameter C_{l_p}, the directional-stability parameters C_{n_β} and $\left(C_{n_\beta}\right)_{DYN}$, and the ratio of the yawing inertia to the rolling inertia I_Z/I_X. These data are for thin delta wings at a lift coefficient of 0.6, but the trends shown are considered to be generally representative of highly swept reentry configurations for a fairly wide lift-coefficient range. The low values of C_{l_p} in the region of sweep angles of about 75° and above, accompanied by large negative values of C_{l_β}, tend to produce poor damping of the lateral or Dutch-roll oscillation; and the high ratio of the yawing to rolling inertia means that the Dutch-roll oscillation becomes practically a pure rolling motion about the body X-axis.

The directional-stability data show that C_{n_β} is low and becomes negative at the higher angles of sweep. The dynamic directional-stability parameter $\left(C_{n_\beta}\right)_{DYN}$, which is defined as $C_{n_\beta} - C_{l_\beta} \frac{I_Z}{I_X} \sin \alpha$, increases rapidly to large positive values at high sweep angles because of the large positive increases in I_Z/I_X and negative increases in C_{l_β}. It has generally been found that the $\left(C_{n_\beta}\right)_{DYN}$ parameter is a better criterion for directional divergence than the static stability parameter C_{n_β}. For example, it has been found possible to fly models with large negative values of C_{n_β} as long as $\left(C_{n_\beta}\right)_{DYN}$ remains positive. (See ref. 4.) In general, the information obtained from figure 7 indicates that Dutch-roll stability problems with highly swept configurations might be expected, but a directional-stability problem would probably not occur.

A comparison of directional stability characteristics for four highly swept glide-landing-type reentry configurations is shown in figures 8 and 9. Figure 8 shows C_{n_β} and $(C_{n_\beta})_{DYN}$ for a delta-wing configuration having a relatively small fuselage and for a right-triangular-pyramid configuration. Both of these configurations have positive values of C_{n_β} over the angle-of-attack range and very large positive values of $(C_{n_\beta})_{DYN}$. Such configurations should have no directional-stability problems. Figure 9 shows data for two reentry configurations of another type - that is, flat-bottom configurations having a large fuselage on top of the wing. This type of configuration generally has static directional instability at high angles of attack but $(C_{n_\beta})_{DYN}$ remains positive. Flight tests of these models showed that they could be flown without any apparent divergent tendency at angles of attack at which C_{n_β} is negative, indicating that $(C_{n_\beta})_{DYN}$ is the significant parameter in these cases.

These directional-stability parameters, however, are not the only factors affecting the directional characteristics. Lateral-control parameters can also be important, as shown by the data of figure 10. The upper part of the figure shows the ratio of yawing moment to rolling moment produced by aileron deflection $C_{n_{\delta_a}}/C_{l_{\delta_a}}$ for the two flat-bottom configurations having a large fuselage on top of the wing. One configuration has wing-tip vertical tails and the other configuration has a single center vertical tail. The data show that aileron deflection produced small favorable yawing moments over most of the angle-of-attack range for the model with the center tail but produced large adverse yawing moments for the model with the wing-tip tails. The large adverse aileron yawing moments are associated with the large induced loads produced on the vertical-tail surfaces by differential deflection of the ailerons. The plot at the bottom of the figure shows that the rudder effectiveness $C_{n_{\delta_r}}$ remained about constant with angle of attack for the center-tail model, but $C_{n_{\delta_r}}$ decreased with increasing angle of attack for the model with the wing-tip tails and became practically zero at 40° angle of attack. At the lower angles of attack the adverse aileron yawing moments of the model with the wing-tip tails could be counteracted by rudder control, but at the higher angles of attack where the rudder effectiveness had dropped off appreciably, the adverse yawing moments produced large yawing motions and the model became uncontrollable. In order to make flights at these high angles of attack for research purposes, additional yawing control was provided in the form of an air jet located at the tail of the model.

The damping-in-roll parameters for four reentry configurations are shown in figure 11. These parameters were measured in forced-oscillation

tests about the body axis so that the parameter is in the form $C_{l_p} + C_{l_{\dot{\beta}}} \sin \alpha$. The data were obtained for a value of the reduced frequency parameter $\omega b/2V$ of 0.1 and for an amplitude of $\pm 5^\circ$. The damping in roll for the thin delta wing with small fuselage on top decreases with increasing angle of attack and becomes unstable. This variation is similar to that of a wing alone. The damping in roll for the other three configurations remains stable with increasing angle of attack.

The calculated Dutch-roll stability for the configurations of figure 11 is presented in figure 12. The reciprocal of the time to damp to one-half amplitude is plotted against angle of attack. The configuration with the thin delta wing has negative Dutch-roll damping in the higher angle-of-attack range while the other three configurations remain stable over the angle-of-attack range. In model flight tests of these configurations, only the variable-geometry configuration was found to have satisfactory Dutch-roll stability without artificial stabilization over the angle-of-attack test range. For the other three configurations the damping was satisfactory at low angles of attack but decreased to unsatisfactory values as the angle of attack increased. At the higher angles of attack, the thin-delta-wing model was found to be unstable as predicted by the calculations. The flat-bottom configuration having a large fuselage on top of the wing was found to be slightly unstable rather than stable. Artificial stabilization was required at angles of attack above 15° for the thin-delta-wing model and above 25° for the other two models.

In order to provide artificial stabilization in the model flight tests, a roll damper has been used in most cases. Figure 13 shows the relative effect of roll and yaw dampers for reentry configurations of the type illustrated in the figure. The reciprocal of the calculated time to damp to one-half amplitude is plotted against values of the damping-in-roll derivative C_{l_p}, the damping-in-yaw derivative C_{n_r}, and the cross derivative C_{n_p}, yawing moment due to rolling velocity. These results show that an increase in $-C_{l_p}$ produced a large increase in the damping of the Dutch-roll oscillation whereas an increase in $-C_{n_r}$ produced only a very small increment of damping. Another point of interest here is that the derivative C_{n_p} also has a large effect on the damping. This effect can be significant in cases where the ailerons used for roll damping produce large yawing moments. In such cases the damper will produce C_{n_p} as well as C_{l_p}, and the C_{n_p} contribution will be stabilizing when the yawing moments are adverse and destabilizing when the yawing moments are favorable.

CONCLUDING REMARKS

It appears that on the basis of the lift-drag ratios and wing loadings now being considered for reentry configurations, the longitudinal characteristics for glide landings should be satisfactory. As for lateral stability, it appears that there should be no directional divergence problems for the reentry types now under study, but many of the configurations are likely to require a roll damper for satisfactory Dutch-roll damping at moderate and high angles of attack. Some configurations with wing-tip vertical tails may have control problems in the form of large adverse aileron yawing moments and low rudder effectiveness.

Although all of the reentry configurations studied to date have low-speed stability and control problems, most of the configurations could probably be developed into reentry vehicles capable of performing satisfactory glide landings.

Langley Research Center,
National Aeronautics and Space Administration,
Langley Field, Va., April 12, 1960.

REFERENCES

1. Weil, Joseph, and Matranga, Gene J.: Review of Techniques Applicable to the Recovery of Lifting Hypervelocity Vehicles. NASA TM X-334, 1960.

2. Moul, Martin T., and Brown, Lawrence W.: Effect of Artificial Pitch Damping on the Longitudinal and Rolling Stability of Aircraft With Negative Static Margins. NASA MEMO 5-5-59L, 1959.

3. Brissenden, Roy F., Alford, William L., and Mallick, Donald L.: Flight Investigation of Pilot's Ability to Control an Airplane Having Positive and Negative Static Longitudinal Stability Coupled With Various Effective Lift-Curve Slopes. NASA TN D-211, 1960.

4. Johnson, Joseph L., Jr.: Wind-Tunnel Investigation of Low-Subsonic Flight Characteristics of a Model of a Canard Airplane Designed for Supersonic Cruise Flight. NASA TM X-229, 1960.

LIFT-DRAG RATIO FOR REENTRY VEHICLES
TRIMMED CONDITIONS

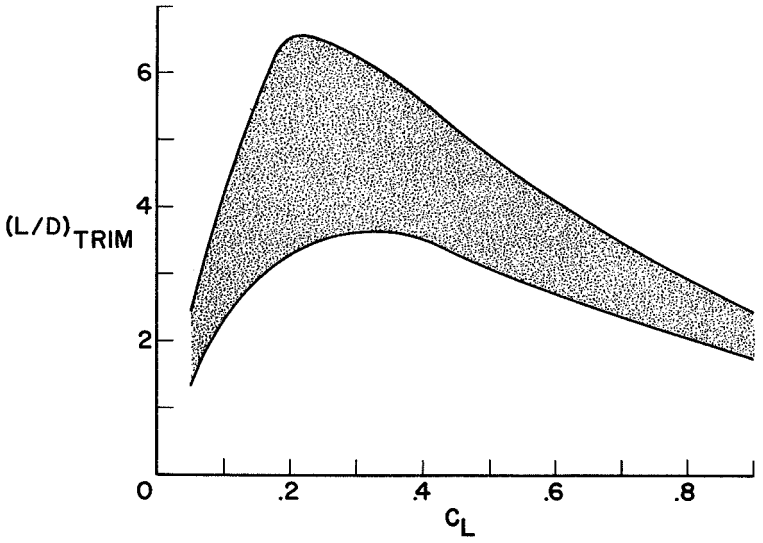

Figure 1

MAXIMUM LIFT-DRAG RATIO
TRIMMED CONDITIONS

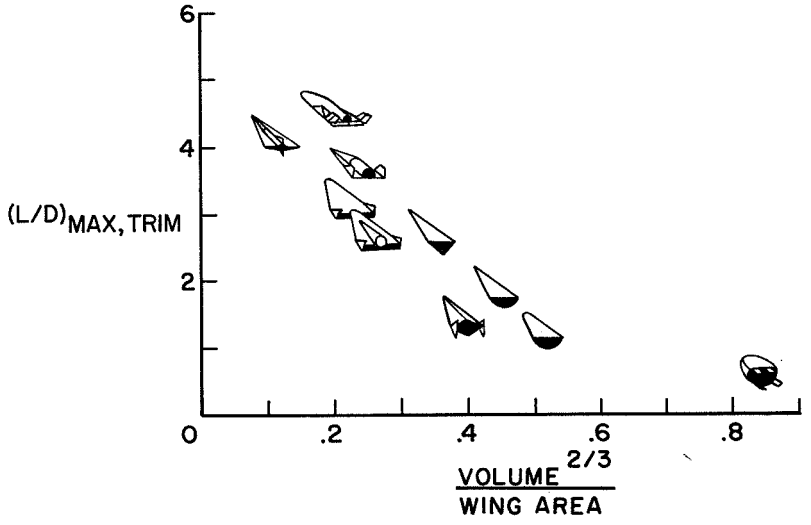

Figure 2

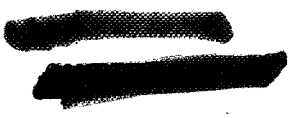

L-1088

CONFIGURATIONS DESIGNED FOR HIGHER LIFT-DRAG RATIO
TRIMMED CONDITIONS

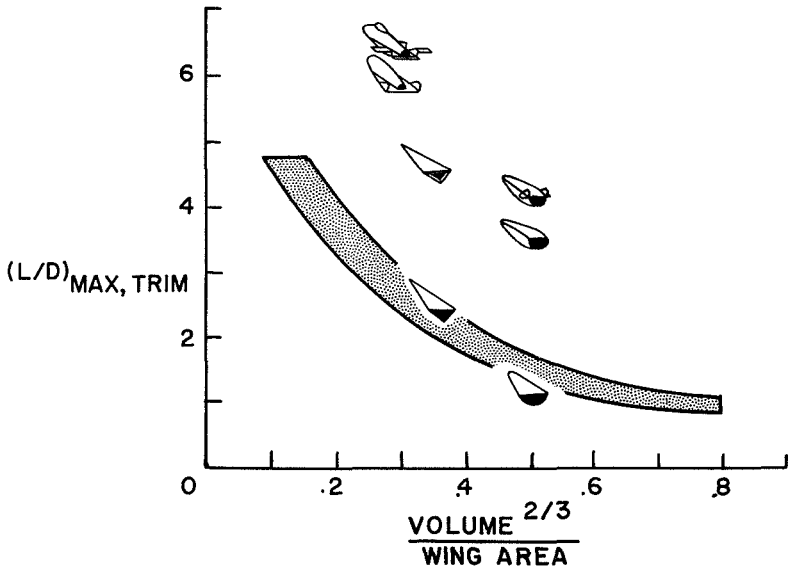

Figure 3

COMPARISON OF L/D FOR REENTRY VEHICLES
AND RESEARCH AIRPLANES
TRIMMED CONDITIONS

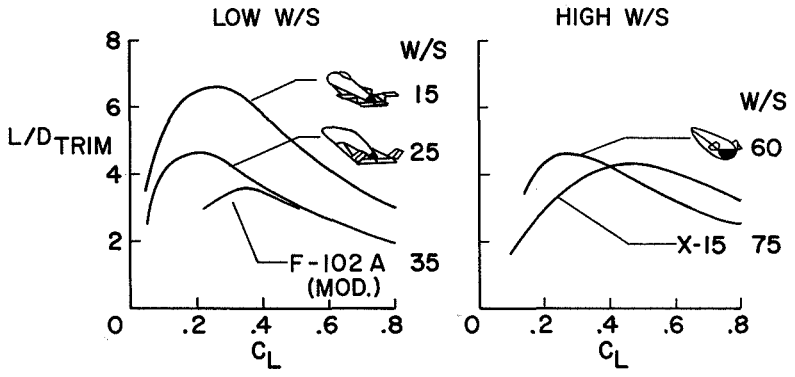

Figure 4

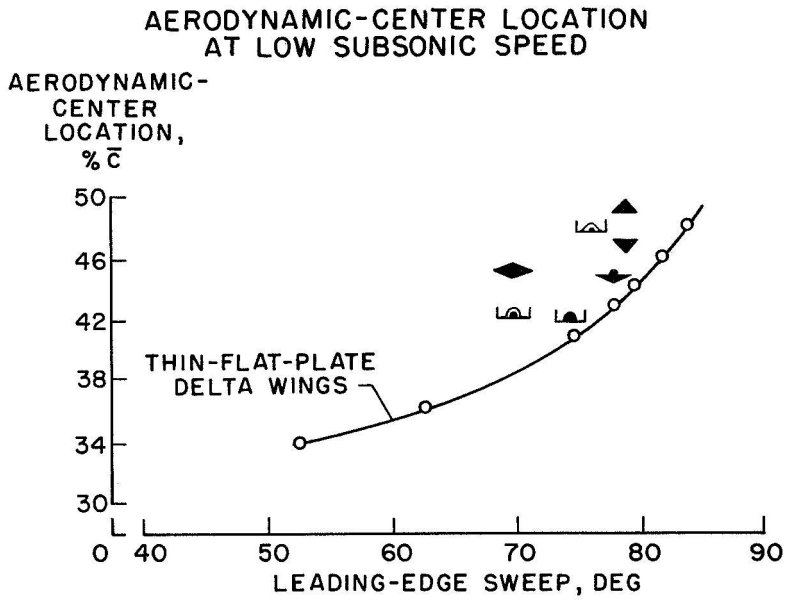

Figure 5

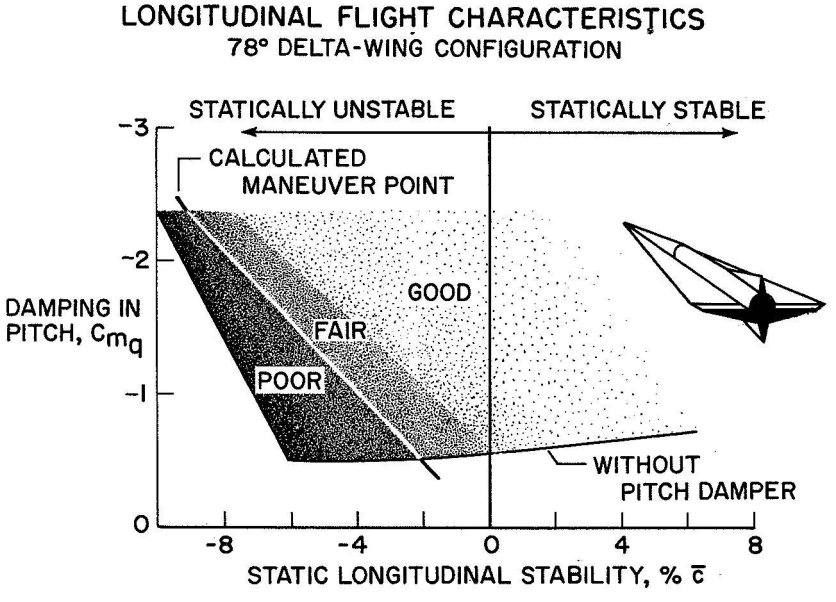

Figure 6

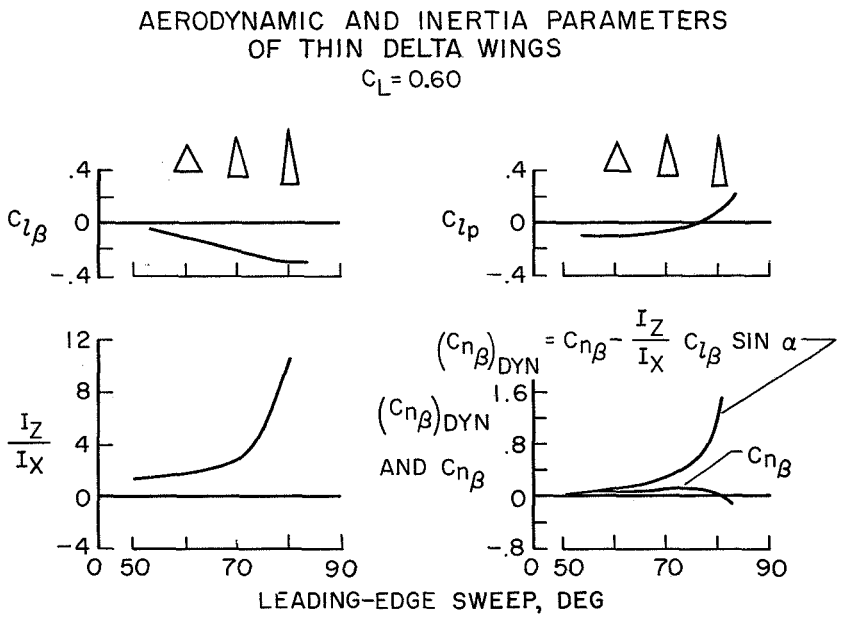

Figure 7

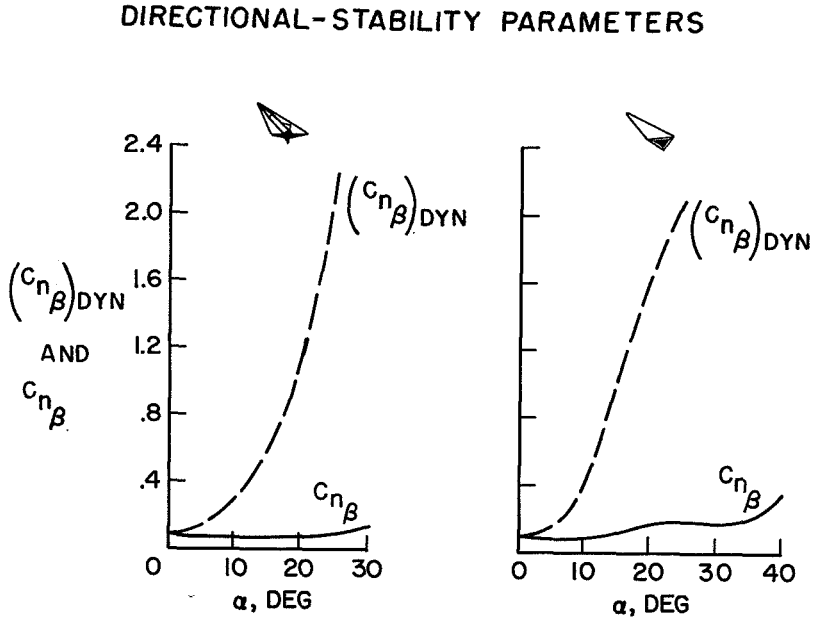

Figure 8

DIRECTIONAL-STABILITY PARAMETERS

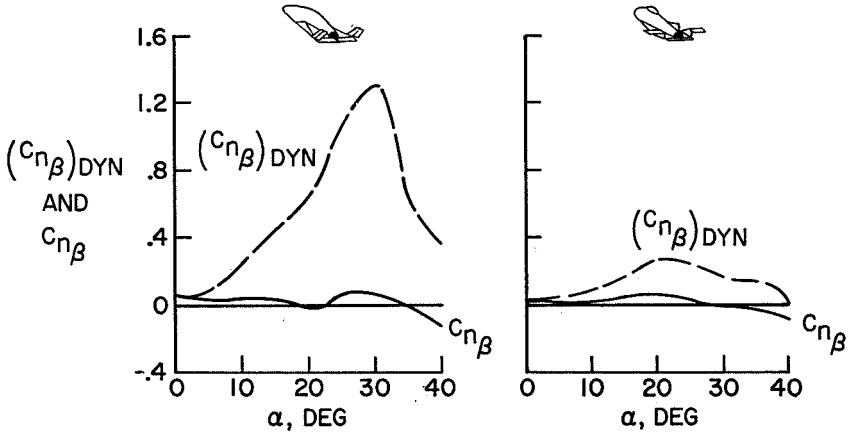

Figure 9

LATERAL CONTROL PARAMETERS

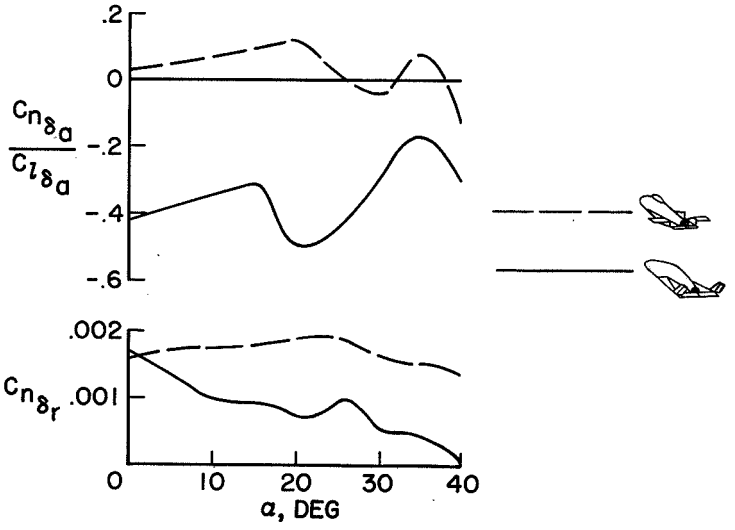

Figure 10

DAMPING-IN-ROLL PARAMETER

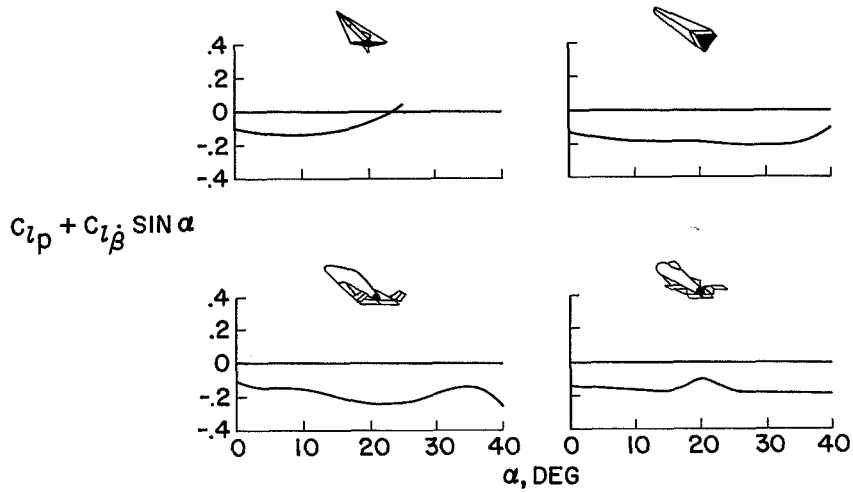

Figure 11

CALCULATED DUTCH-ROLL STABILITY

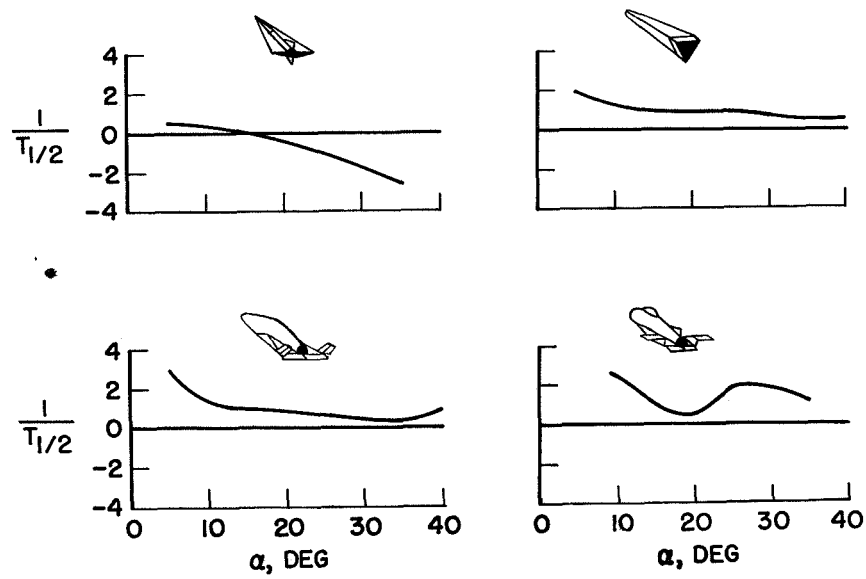

Figure 12

EFFECT OF C_{l_p}, C_{n_p}, AND C_{n_r} ON CALCULATED DUTCH-ROLL STABILITY

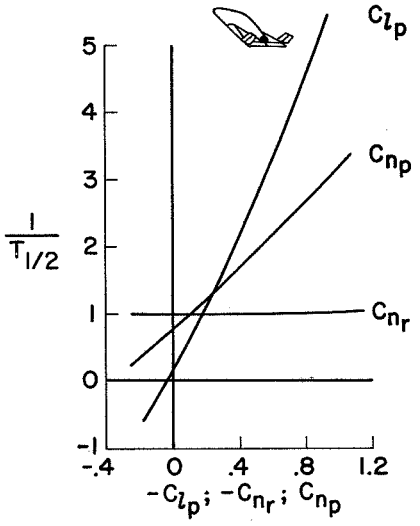

Figure 13